AIAA 92-0331
Initial Operation of the UTA Shock Tunnel

F.K. Lu
University of Texas at Arlington
Arlington, TX

30th Aerospace Sciences Meeting & Exhibit
January 6-9, 1992 / Reno, NV

AIAA 91-0331

Initial Operation of the UTA Shock Tunnel

Frank K. Lu†
The University of Texas at Arlington, Arlington, TX 76019-0018

A small shock tunnel has recently been put into service in a university environment. The shock tunnel has been used for high Reynolds number, perfect gas simulation of hypersonic flow. Tradeoffs between various constraints to achieve the test requirements are discussed. Methods for obtaining precise control of test conditions and for protecting low-range pressure transducers from overpressure damage are described. Present research activities are also briefly discussed.

Introduction

The heyday of hypersonic research in the 1950s and 1960s was precipitously followed by a period of slump with dwindling resources and interest in hypersonic flows. As is now obvious, many test facilities were shut down, mothballed or scrapped. Thus, in the U.S., there were only 19 hypersonic facilities in 1985 compared against 82 in 1963 [1]. A renaissance of sorts has, however, occurred, this renaissance being spurred by a variety of new hypersonic programs. Wittliff's compilation [1] showed that there were 24 hypersonic facilities in 1987 in the U.S., up from that in 1985.

The hypersonic scenario in the 1990s is vastly different from that in the 1950s. One must recognize the advent of computational fluid dynamics, new diagnostic capabilities and "computer-aided experimentation." Also, testing requirements are different. Current interest in sustained hypersonic airbreathing flight has provided challenges in devising ways of testing combustion systems and has sparked the development of facilities that can provide adequate simulation [2]–[4].

The renewed interest in hypersonic aerodynamics prompted the University of Texas at Arlington (UTA) to start a modest experimental research program through construction of a shock tunnel [5, 6]. The tunnel design is partly based on the NASA-Langley Expansion Tube Facility [7], which has been extensively re-fitted and presently located at the General Applied Science Laboratories, Inc., Ronkonkoma, New York [4] where it is known as the HYPULSE. From preliminary design in 1986, the tunnel was ready in mid-1989, with shakedown tests completed by early 1990. This paper describes initial experiences in operating the tunnel. Efforts at applying the tunnel for high Reynolds number, perfect gas testing and for boundary-layer studies will be discussed in this paper. Before discussing the operational experiences, however, the tunnel facility, together with special improvements, will be briefly described. The paper concludes with a discussion of ongoing and proposed research.

†Assistant Professor, Aerodynamics Research Center, Aerospace Engineering Department. Senior Member AIAA.

Facility description

The UTA shock tunnel is housed in the Aerodynamics Research Center (ARC) which is a two-building complex. In the main building are the hypersonic shock tunnel, a transonic Ludwieg tube, a closed-circuit low-speed tunnel and an arc-heated tunnel, which is presently under development. There are also a central control room, a computer room, a model shop, an electronics shop and an office wing. In an auxiliary building are a Clark CMB-6 5-stage air compressor that can supply 24 MPa (3,500 psi) dried air at 0.95 m^3/s (2,000 scfm) STP conditions and an Ingersoll-Rand 15T2 compressor rated at 6.9 MPa (1,000 psi). The Clark compressor is derated to operate at 14.5 MPa (2,100 psi) to match the pressure rating of the storage bottles.

A partial view of the UTA shock tunnel is shown in Fig. 1. The tunnel is of conventional design and, as can be seen in sequence from the top of Fig. 1, consists of a test section, a nozzle and a shock tube. Only part of the driven section of the shock tube is visible in the figure. Partly hidden from view is the diffuser which protrudes out of the far wall into a vacuum tank outside. Not visible are a double-diaphragm section and the driver section of the shock tube. In addition to the tunnel itself, the figure also shows the data acquisition crate on the left and the vacuum system on the right. Brief descriptions of the major components will now be given.

Shock tube

The shock tube consists of a high-pressure driver tube connected to a driven tube by a double-diaphragm section. The driver tube has a bore of 152 mm (6 in.) and is 3 m (10 ft) long. The driven tube also of 152 mm (6 in.) bore is made of three 2.7-m (9-ft) segments to facilitate installation and disassembly, when necessary for cleaning. The driver tube and the three driven-tube segments are rated for a pressure of 41 MPa (6,000 psi).

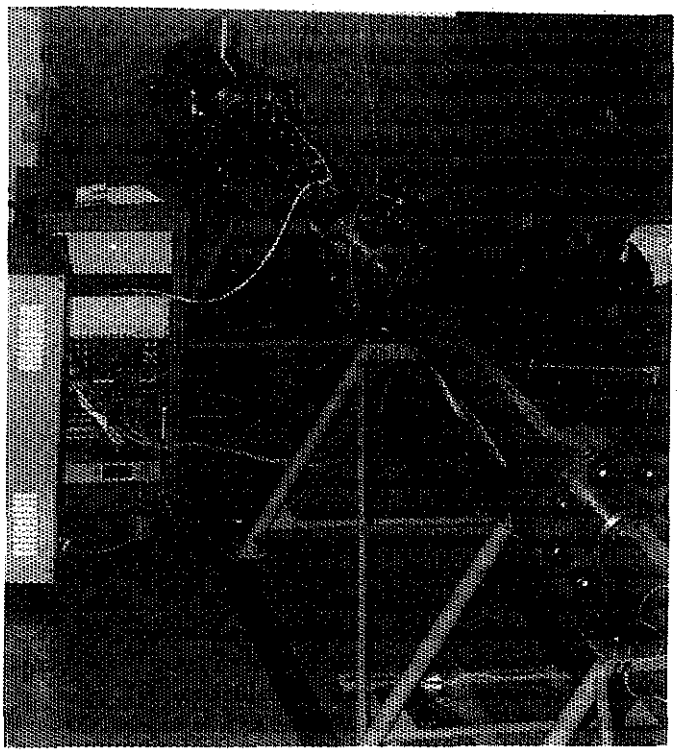

Figure 1: The UTA shock tunnel.

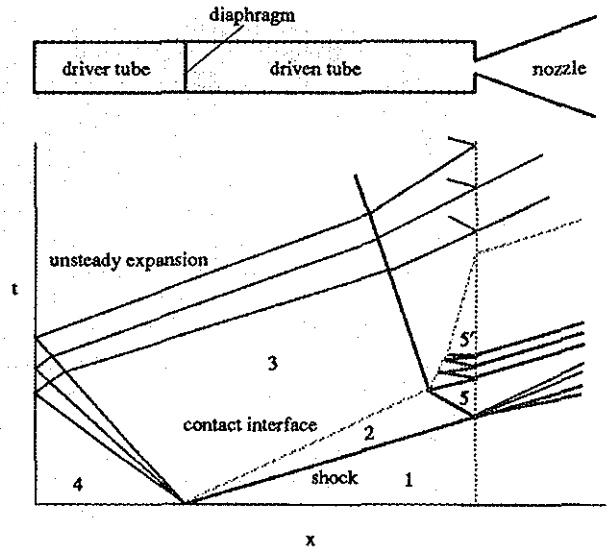

Figure 2: Shock tube schematic and regions in an ideal wave diagram.

The driver tube, the diaphragm section and the driven tube are bolted together with two diaphragms enclosing a plenum. The upstream faces of the diaphragm section and the driven tube have rounded inside corners. The rounded corners allow the diaphragms to stretch when subjected to high pressures and help to prevent uncontrolled and unexpected diaphragm failure through shear if the corners were sharp.

To replace the diaphragms, the driven tube is unbolted from the double-diaphragm section and the driver tube, and then rolled away using a hydraulic jack. However, reassembling the pieces is not so straightforward since the driver tube may shift slightly from the tunnel axis. To ensure proper fit of the parts on reassembly, tapered guide pins located on the upstream faces of the diaphragm section and driven tube mate into countersunk holes in the opposing faces.

Diaphragms

It is common in shock-tube practice to use double diaphragms enclosing a plenum chamber for precise control of diaphragm rupture. A double-diaphragm arrangement is also used for the UTA shock tunnel. The diaphragm material currently in use is 10-gauge (3.42 mm, 0.1345 in.) hot-rolled steel sheets (ASTM A36) 267 mm (10.5 in.) square, chosen because of its low cost.

To operate the tunnel, the plenum between the driver and driven tubes is charged to a pressure of about $0.5p_4$. (The nomenclature p_1 etc. are shown in a wave diagram in Fig. 2 and follows convention.) The tunnel is fired by venting the plenum chamber. Venting the plenum eventually causes the upstream diaphragm to rupture since this diaphragm is subjected to a large pressure difference between its faces. The downstream diaphragm subsequently fails when subjected to a similar large pressure difference.

Further, it is also usual practice to score a pattern onto the diaphragm to ensure clean rupture with minimum fragmentation while also providing a degree of controllability. The diaphragms are drilled for bolting to the tunnel before being scored with a router using a custom-built rig as shown in Fig. 3a. A *cross potent* pattern 3.18 mm (0.125 in.) wide and 0.5 ± 0.1 mm (0.020 ± 0.005 in.) deep is found to give optimal diaphragm opening, Fig. 3b [9]. An almost similar pattern was used by Needham et al. [8]. A simple cross is found to be unsuitable for our purpose since it often results in partial opening of the diaphragms or, even worse, fragmentation of large pieces of material which may be discharged into the test section.

The router allows diaphragms to be made cheaply and quickly compared to stamping, milling or chemically etching the patterns because the double-diaphragm operation does not require stringent tolerances on the scoring depth. The diaphragms, as made using the rig shown in Fig. 3a, fail when subjected to a pressure difference of about 13 MPa (2,000 psi), which is larger than the initial pressure difference that the diaphragms are subjected to in the shock tube. Also,

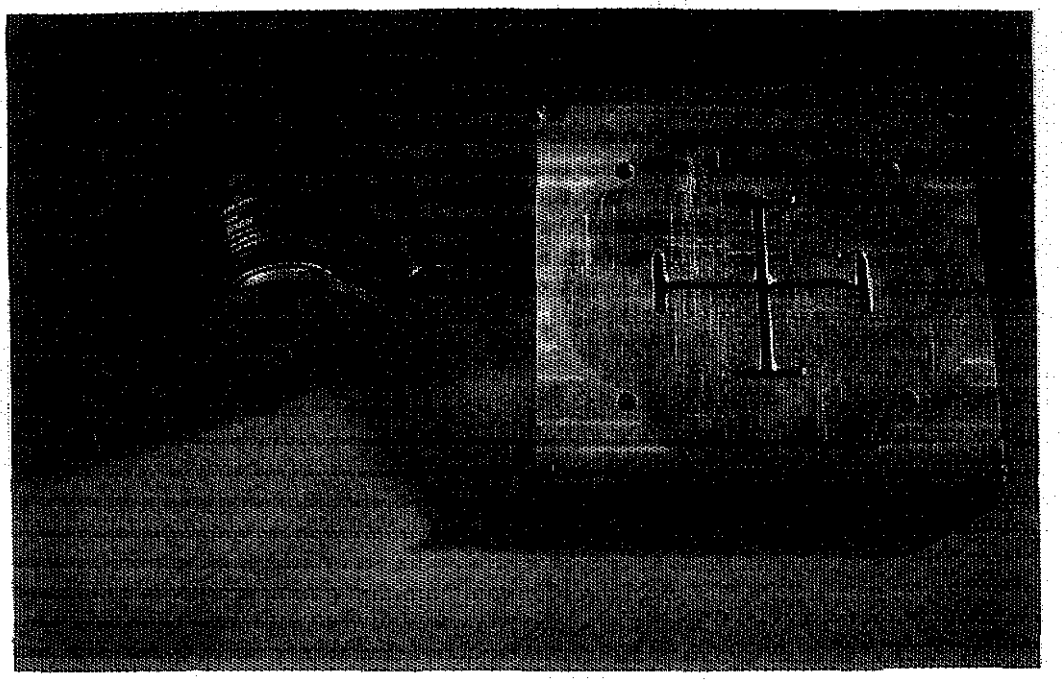

a. Diaphragm scoring rig, router at left and scoring template at right of photograph.

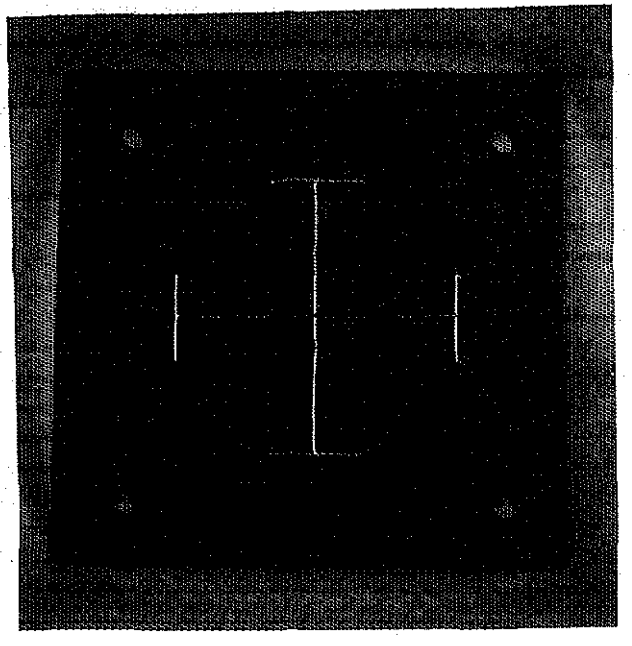

b. New diaphragm.

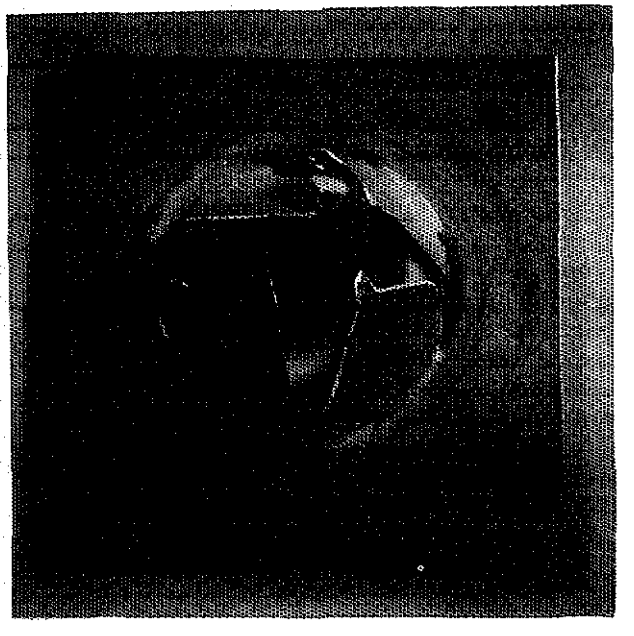

c. Used diaphragm.

Figure 3: Photograph of diaphragm scoring rig, and new and used diaphragms.

to cut cost and speed up the diaphragm manufacturing process, the diaphragms do not have a ring flange to restrain them from being pulled and deformed when subjected to pressure loading as reported in Refs. [7, 10]. The diaphragms in our operation are in fact allowed to stretch and deform. A small test program was conducted to ensure that such a technique can be applied safely and an accurate correlation was obtained between score depth and rupture pressure. It may be noted that the diaphragms are placed in the tunnel with the scoring pattern facing downstream.

The diaphragms generally "petal" without fragmentation, Fig. 3c. Sometimes, the petals face upstream or are curled after rupture. These are likely due to shock reflections in the shock tube. Further, in the extremely unlikely occurrence of fragmentation, the few fragments tend to be small and are trapped in the driven tube. These small fragments are cleaned out in preparation for the next run.

Nozzle, test section, diffuser and vacuum tank

The nozzle, test section and diffuser were donated to UTA by LTV Aerospace and Defense Co., Dallas, Texas. A 7.5° half-angle conical nozzle with interchangeable throat inserts enables test Mach numbers of 5 through 16 to be obtained. The exit diameter of this nozzle is 336 mm (13.25 in.). Presently, a Mach 8 throat insert is used. A second, Mach 8 contoured nozzle of 200 mm (7.85 in.) exit diameter, and associated test section and diffuser are also available but have not been used.

A secondary diaphragm made of 0.127-mm (0.005-in.) thick aluminum sheet is located in the nozzle throat region and is used to separate the driven-tube gas from that in the test section. The secondary diaphragm is not scored. The test section is of semi-free jet design, 536 mm (21.1 in.) long and 440 mm (17.5 in.) in diameter. The nozzle and the diffuser both protrude slightly into the test section. On either side of the test section are two 230 mm (9 in.) diameter access ports that are equipped with schlieren-quality windows for flow visualization. Instrumentation and mounting ports are also available through the floor of the test section and the floor and roof of the diffuser. Downstream of the diffuser is a 4.25-m^3 (150-ft^3) vacuum tank designed for a pressure of up to 550 kPa (80 psia).

Pneumatic systems

Compressed air is cooled and dried before storage in bottles totaling 4.25-m^3 (150-ft^3). About ten minutes are required to charge the bottles. (Although provision for helium charging is available, testing thus far has used high-pressure air.) High-pressure air is piped to different locations of the ARC via an elaborate distribution system [5]. For the shock tunnel, the air is further compressed by a Haskel Model 55696 two-stage booster pump adjacent to the tunnel up to a maximum pressure of 41 MPa (6,000 psi). Testing thus far has been with air stored at 31 MPa (4,500 psi) only. The stored air is then regulated to lower pressure when charging the driver and driven tubes. A system of manual and remote-control valves is used to operate the tunnel's high-pressure system [6].

In addition to the high-pressure system, a vacuum system is installed. A Sargent-Welch Model 1376 vacuum pump is used to evacuate the driven tube while a Sargent-Welch Model 1396 vacuum pump is used to evacuate the test section and vacuum tank. A custom-made pressure relief valve is incorporated into the vacuum tank to protect low-range pressure transducers. This valve consists of a circular plate sealed tightly against a 76 mm (3 in.) pipe flange when the vacuum tank is evacuated. The seal is broken when the pressure in the vacuum tank exceeds atmospheric causing the circular plate to pop from the flange and move along guide rods. After all pressure is relieved, the valve is manually closed for the next run. This simple yet effective approach has protected 0–35 kPa (0–5 psia) transducers and microphones from overpressure damage. Previously, 0–350 kPa (0–50 psia) transducers had to be used, with a resulting loss of resolution when measuring low pressures.

Data acquisition system

The data acquisition system consists of a LeCroy Model 1434A CAMAC (IEEE-583) mainframe housing a Model 8901A Interface (GPIB, IEEE-488 ↔ CAMAC, IEEE-583), two Model 6810 and one Model 8212A digitizer, and a Model 8800A memory module (32 kbytes). The two Model 6810 modules of four channels each can acquire data simultaneously from 20 samples per second up to five million samples per second, the maximum sampling rate being dependent on the number of active channels. These modules can store 512 kbytes of data each. Usually, in the experiments, all eight channels are used simultaneously at the maximum possible rate of one million samples per second per channel. The lower speed (0.2–40 kilosamples per second) 32-channel Model 8212A digitizer with the Model 8800A memory module is also available for connecting to sensors used to monitor tunnel performance. Eight external instrumentation amplifier-filter combinations (Leyh Model 29) are available to condition the incoming high-speed data. These are usually operated with a gain of 500 and a bandwidth of 100 kHz. The data acquisition system is connected to an Everex Step 286 microcomputer via a pair of National Instruments Model GPIB-100 bus extenders since the microcomputer is located in a reinforced control room over 30 m (100 ft) away. Finally, a number of software is available for controlling

the data acquisition system and for processing data.

Instrumentation and diagnostics

A variety of Kulite and PCB pressure transducers, Medtherm coaxial thermocouples and Omega bead thermocouples is available for monitoring the tunnel and for performing research. These transducers and thermocouples can be calibrated dynamically using a shock tube located by the shock tunnel.

For Kulite piezoresistive-type pressure transducers, the author's experience has been that a static calibration suffices for determining their sensitivities even though these transducers are used in dynamic situations [11]. But the drift and hysteresis of these transducers can be significant, especially if the transducers are used to measure low pressures [12]. To reduce drift, the transducers are calibrated in situ against an MKS Baratron Model 127A vacuum gauge, a capacitance-type manometer accurate to ± 7 Pa (± 0.001 psia), used widely as a secondary standard. The calibration is performed during evacuation of the test section. Least-squares linear fits are made to the calibration data from which the transducers' sensitivities are obtained. About 30 minutes elapse between a run and the calibration during which significant zero shift is encountered. The drift problem is overcome by "renulling" the transducers by comparing their outputs against the vacuum gauge prior to tunnel firing. Subsequently, the acquired data are converted into engineering units using a first-order fit, with the sensitivities obtained from calibration and the offsets obtained from the final renulling adjustment. Other problems of piezoresistive transducers, namely, thermal zero shift and thermal sensitivity are negligible due to the short run times of the tests.

Heat transfer measurements in the shock tunnel are made using coaxial thermocouples [13, 14] with sensing surfaces of 1.55 mm (0.061 in.) diameter. The thermocouples can be shaped to conform to the contour of a model and are also extremely fast in response, the response being estimated by the manufacturer to be in the microsecond range. In the short duration of a run, the coaxial thermocouple can be modeled as a one-dimensional semi-infinite solid whence the thermal penetration depth is small compared to the thermocouple dimensions. In other words, the Fourier number $Fo \equiv \alpha t/d^2$ must be less than 0.5 for the small penetration depth assumption to be applicable [13]; α = thermal diffusivity, t = time and d = thermocouple diameter. Further, in the present implementation, chromel-constantan thermocouples are placed in stainless steel models since the thermocouple materials have approximately the same value of the thermal product $\sqrt{\rho C K}$, where ρ = density, C = specific heat, K = thermal conductivity, as stainless steel so that the thermocouples appear nearly "transparent" [13]. The thermocouples are insulated electrically from the model by a thin coat of silicone rubber, which also acts as a shock absorber [15]. In the past, data reduction techniques involved the use of analog circuitry to obtain the heat transfer rate from dynamic measurement [16]. With the rapid data acquisition system available to the shock tunnel, the digitized data are reduced numerically and dispense with excessive electronic hardware [17].

A pitot rake and a boundary-layer rake are available to the shock tunnel. The pitot rake is of conventional design, with a pentagonal cross section. A 10° semi-angle sharp wedge forms the front of the rake housing while the back is of rectangular section. The housing is 70 mm (2.75 in.) long and 12.7 mm (0.5 in.) thick and can accomodate a maximum of 13 probes, consisting of Kulite transducers or thermocouples encased in stainless steel tubes, in 1.5-mm (0.06-in.) diameter holes spaced 12.7 mm (0.5 in.) apart. The pitot rake is mounted on a sting which can be traversed from the nozzle into the diffuser, and can also be rotated and offset from the tunnel centerline.

The boundary-layer rake consists of a 130 mm (5.125 in.) long, 57 mm (2.25 in.) high by 22 mm (0.875 in.) wide hollow housing with a streamlined nose. In front of the housing are machined two slots, 38 mm (1.5 in.) high by 3.2 mm (0.125 in. wide), on either side of the plane of symmetry. One of the slots is for an array of pitot probes and the other is for an array of thermocouples. Usually, a stack of three pitot and another stack of three thermocouple probes are inserted into a movable subhousing within the main housing. The probes protrude through the slots and can be moved in small albeit variable steps to build up a boundary-layer profile in about four runs. After positioning the probes, a set screw is tightened against the subhousing to lock the probes in place. The pitot probes for boundary-layer surveys are flattened as is typical. To obtain adequate response, Kulite transducers are placed 18 mm (0.7 in.) from the tube orifices. The thermocouples are exposed to the incoming stream and are used for estimating stagnation temperature using a heat transfer method [18]. The boundary-layer rake is mounted to a flat plate using a number of adapters for on- and off-centerline surveys. Also, angled adapters are available to survey the flow past expansion corners.

In addition to transducers and thermocouples, the shock tunnel has a schlieren system, on permanent loan from Bell Helicopters Textron, Fort Worth, Texas. The system consists of a pair of 300-mm (15-in.) diameter spherical mirrors with focal lengths of 2.44 m (96 in.), mounts, knife edges, strobe light and camera.

Tunnel operation

A key parameter in shock tunnel operation is the Mach number of the shock propagating through the driven tube M_s. For real gas simulation, a high value of M_s is

desired. Briefly, this is achieved by using a light driver gas (e.g., helium or hydrogen), by heating the driver gas, or by a combination of heating and compressing a light driver gas using a piston [19]. But, at present, the UTA shock tunnel is used for high Reynolds number, perfect gas testing. The technique for achieving this requirement will be described following a brief discussion of present tunnel operation at UTA. (For a review of shock tunnel principles, see Ref. [20].)

The tunnel is operated in the reflected shock mode as shown schematically in the ideal wave diagram of Fig. 2. Bursting the double diaphragm causes the driver gas to expand into the driven tube which generates a normal, primary shock. Downstream of this shock and just ahead of the contact surface separating the test gas from the driver gas is region 2 in the wave diagram of Fig. 2, with high temperature and high pressure. The primary shock is reflected at the end of the driven tube, which gives rise to the nomenclature "reflected mode" being used to describe this type of operation, the tiny orifice of the nozzle at the end of the driven tube being negligibly small to a first approximation. The reflected shock further compresses and heats the test gas into the stagnant region 5. This compressed, heated gas is then expanded by the nozzle to the test conditions.

The reflected mode has a longer run time as opposed to the non-reflected mode in which the shock propagates into the nozzle. The run time in the reflected mode, however, is governed by wave interactions in the driven tube. The test time is terminated either by the arrival of the contact surface or the unsteady expansion wave at the driven-tube face. Further, if the initial pressures and temperatures of the driver- and driven-gases are such that the reflected shock is not further reflected by the contact surface but is totally transmitted through a "transparent" interface, the tunnel is said to be operated under "tailored interface" conditions. Tailored operation gives the longest achievable test time compared against untailored operations but is achieved by a unique set of initial conditions for given test requirements. This set of initial conditions may be difficult or expensive to obtain in practice.

Forsaking tailored interface operation provides greater flexibility of tunnel operation at the expense of shorter test times, a situation which may not be too adverse if high-speed data acquisition systems are available. The primary reflected shock is only partially transmitted at the contact surface and either an unsteady expansion wave or a secondary shock is reflected. The former is known as "undertailoring" while the latter is known as "overtailoring," and is the case illustrated schematically in the wave diagram of Fig. 2. The overtailored condition is sometimes known as the "equilibrium interface" mode of operation and is the way that the UTA shock tunnel is operated at present to achieve high Reynolds number, perfect gas testing at Mach 8 in a cost-effective and efficient way. Ref. [21] has a recent discussion of tailored interface operation. The equilibrium interface operation will be further discussed later when discussing the useful run time of the tunnel. The choice of specific initial conditions in the equilibrium interface operation is governed primarily by the high Reynolds number, perfect gas requirement of ongoing research, and is obtained at the sacrifice of some test time as may be apparent when compared against the tailored interface mode of operation. The way that the high Reynolds number, perfect gas conditions are achieved will be described next.

High Reynolds number, perfect gas testing

To achieve (nearly) perfect gas conditions in air, the stagnant test gas in region 5 (Fig. 2), after shock compression, should be under as high a pressure p_5 as possible and also be at a high temperature T_5 which is subjected to two limits. The upper limit on T_5 is set by the perfect gas requirement while the lower limit is set by the liquefaction of air in the test section for a given Mach number. Based on the above considerations, although the tunnel's preliminary performance estimates relied on viscous and real gas computer codes [6], condition 5 was obtained using classical quasi-steady, one-dimensional inviscid shock-tube theory and some results of the inviscid calculations are shown in Figs. 4 and 5. The calculations assume that air is used throughout. The figures show the data in dimensional form for clarity and are thus specific to the present tunnel geometry.

Fig. 4 shows that the unit Reynolds number Re is less sensitive to p_4 than to p_1. It was decided that $Re \approx 10^7\,\mathrm{m}^{-1}$ represents the lowest acceptable unit Reynolds number at Mach 8, based on the test conditions of other existing hypersonic facilities [1, 22]. (With this design value of Re, a long flat plate is used to generate a turbulent boundary layer as will be described later.) The chosen value of Re sets p_1 at 276 kPa (40 psia). A choice of p_4 is still available. The next criterion applied is the tunnel static temperature T_{t_s} at Mach 8, which is chosen as 66 K (120 °R), an acceptable static temperature for hypersonic tunnel testing using air, as can be seen from tunnel characteristics summarized in Ref. [22], for example. Further, the static pressure and temperature values should result in negligible liquefaction [23]. But the requirements of high Reynolds number and high static temperature, if the latter is also desirable, are in conflict. Although elaborate ways are available to resolve the conflicting requirements [19], these were not implemented since they were deemed unnecessary, at least for the moment. From Fig. 4, it can be seen that $T_{t_s} \approx 66\,\mathrm{K}$ can be obtained with $p_4 \approx 25\,\mathrm{MPa}$ (3,600 psia). Also, from Fig. 5, the stagnation temperature is about $T_5 = 920\,\mathrm{K}$ (1660 °R) which is low enough to satisfy the perfect gas require-

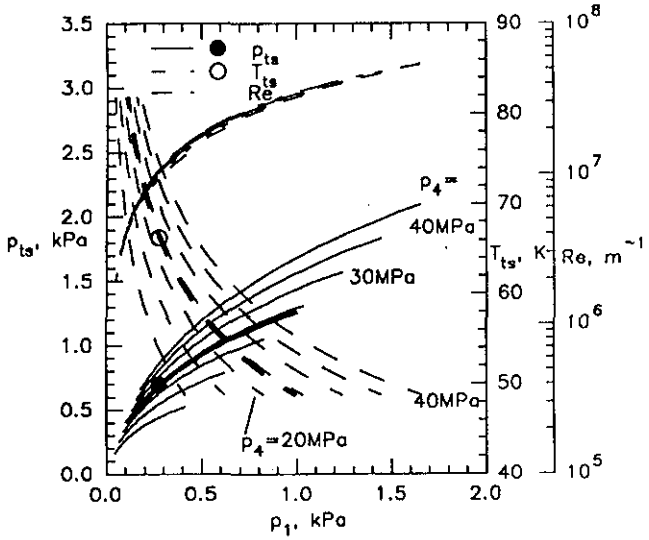

Figure 4: Test section conditions based on inviscid shock-tube theory.

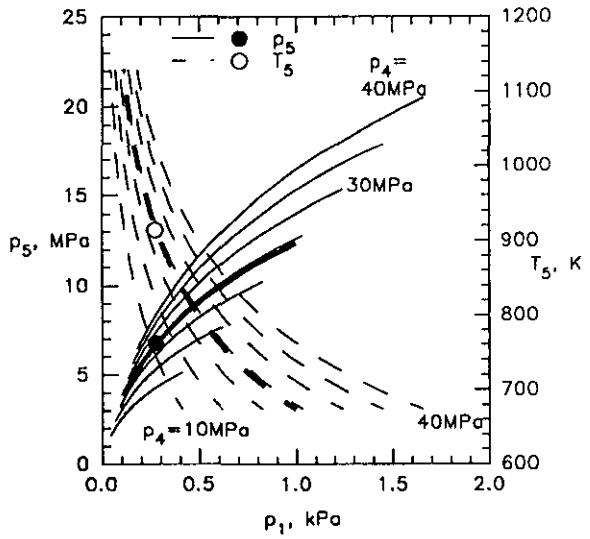

Figure 5: Stagnation conditions based on inviscid shock-tube theory.

ment. In practice, the driver pressure is set to 24 MPa (3,500 psia) instead. This condition is shown as thick lines in Figs. 4 and 5. With a driver pressure of 24 MPa, one charge of the pressure vessel to 31 MPa (4,500 psia) is sufficient for two runs.

Having estimated the tunnel performance, a series of experiments was performed to check the calculations. Fig. 6 shows pressure traces obtained 610 mm (24 in.) from the end of the driven tube and in the test section, the latter on a flat plate. It can be seen that the average stagnation pressure is only $p_5 = 5.4$ MPa (780 psia), below the inviscid prediction of 7 MPa. Calculations based on measurements of $M_s = 2.15 \pm 5\%$ also confirm the measured values of p_5 and, further, provide calculated values of T_5 as approximately 820 K (1,480 °R), resulting in $Re \approx 10.2 \times 10^6\,\mathrm{m}^{-1}$ (3.1 million/ft). Expanding the flow to Mach 8 results in a static pressure and static temperature of 550 Pa (0.08 psia) and 60 K (108 °R) respectively, which are above the air saturation line [23].

Turbulent boundary layer

It is well known that the transition Reynolds number increases with Mach number. In hypersonic testing of turbulent boundary-layer flows, long models are, therefore, unavoidable. Although artificially tripping the boundary layer to shorten the model may appear feasible at first, this is not recommended for fundamental research since disturbances caused by the trips are convected for long distances downstream [24]. Consequently, the mean boundary-layer properties may appear to be those of a turbulent one but the fluctuating properties may not, in fact, be in equilibrium. To obtain a turbulent boundary layer, a long flat plate without trips is used in the shock tunnel. The flat plate is 200 mm (8 in.) wide by 960 mm (37.75 in.) long and has a 15°-sharp leading edge. It is mounted with the top 50 mm (2 in.) below the tunnel midplane. By mounting the flat plate below the tunnel midplane, the boundary layer of approximately 12 mm (0.5 in.) thick is not seriously affected by the focusing of Mach waves onto the tunnel centerline, a phenomenon that exists in axisymmetric tunnels, especially those with conical nozzles [25].

The flat plate used for boundary-layer studies is designed with flexibility in instrumentation as a primary feature. The flat plate shown in Fig. 7 is constructed as follows. A 12.7-mm (0.5-in.) thick aluminum base is hollowed out on top for instrumentation and ancilliary wiring, the wiring being channeled through a port in an end cap bolted to the rear. On this base are attached 12.7-mm (0.5-in.) thick stainless steel plates, typically 200 mm (8 in.) square. These "segments" incorporate grooves lined with "O"-ring material and are butted against each other tightly to provide a smooth test surface. To maintain structural integrity, the leading-edge segment which has a sharp leading edge is usually not removed from the aluminum base. "Skirts" or rails made of 25-mm (1-in.) square stainless steel rods with pointed upward-curving tips are attached along both sides of the model, serving to prevent crossflow contamination from the lower surface. These rails have tapped holes that can be used to attach models and probes. The entire assembly is mounted onto a pedestal which in turn is bolted to the floor of the test section.

Preliminary estimates of transition length were obtained from Refs. [26, 27]. The end of transition was estimated to be at most 330 mm (13 in.) from the flat-plate leading edge. Thus, experiments involving turbulent boundary layers were conducted further downstream, starting at 750 mm (29.5 in.) downstream of the flat-plate leading edge. Boundary-layer surveys were attempted at the test region using pitot and stagnation temperature rakes and will be reported soon.

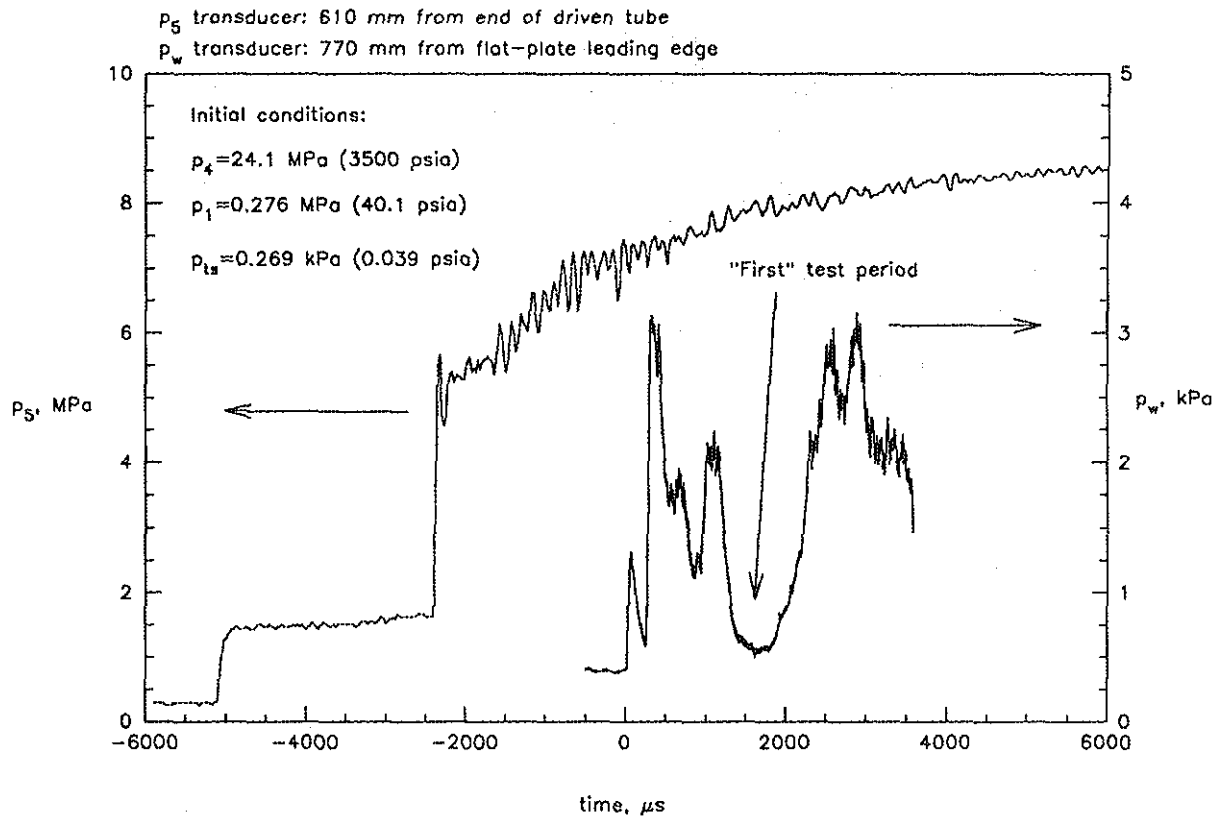

Figure 6: Pressure traces.

Figure 7: Flat plate.

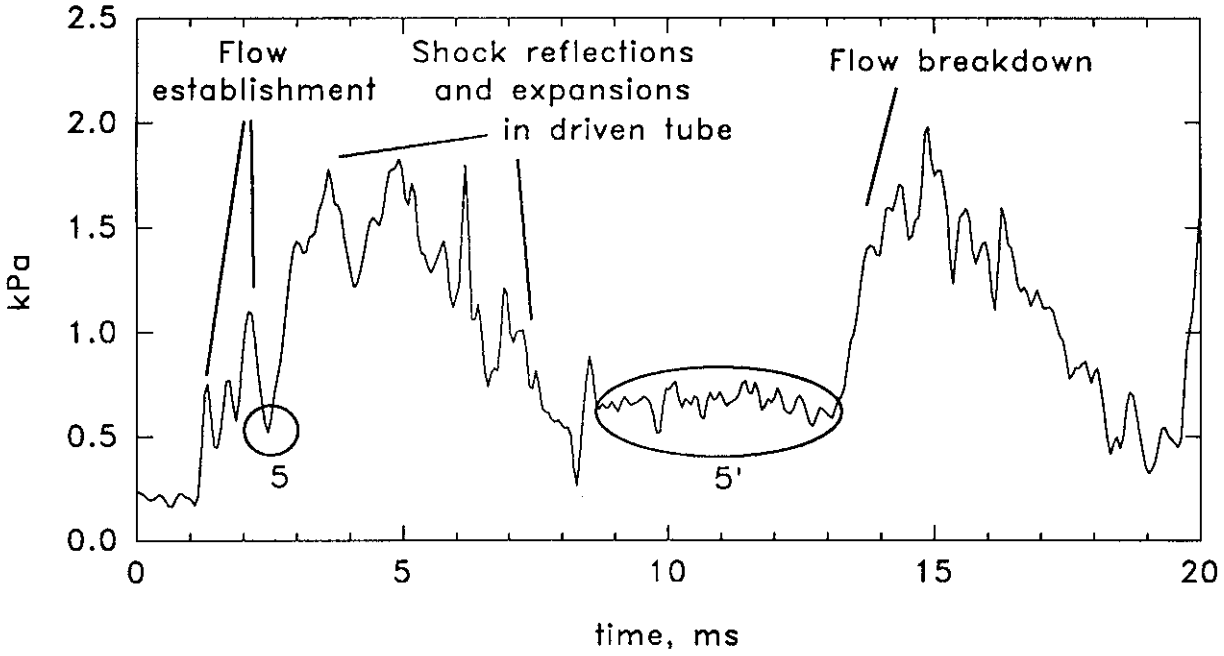

Figure 8: A long pressure trace showing test times given by conditions 5 and 5′.

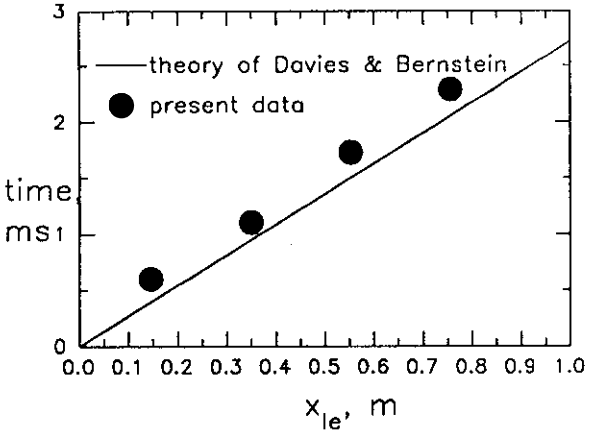

Figure 9: Flow establishment on test model.

Useful test time

Without elaborate operational techniques to achieve tailored conditions, the high Reynolds number requirement could only be satisfied by operating the tunnel in an overtailored condition as discussed previously. In the overtailored mode of operation, the primary shock, upon reflection at the end of the tube, is partially reflected and partially transmitted as it interacts with the contact interface. The secondary reflected shock then strikes the end of the driven tube and traps a stagnant region of gas, labeled 5 in Fig. 2. This gas is accelerated by the nozzle, providing a useful test time of 0.3–0.5 ms, the actual test time being highly dependent on the unsteady wave system set up past the test configuration. Further reflections of the secondary shock compress the test gas to produce another useful test period, labeled 5′ in Fig. 2. This test period is about 3–5 ms long and is terminated by the arrival of either the driver gas or the unsteady expansion after its reflection from the end of the driver tube. Thus, two test periods are available per run as can be seen in Fig. 8 which is an example of a long data record obtained from a pressure transducer mounted on the flat plate.

Certain interesting portions of the pressure history record of Fig. 8 have been labeled. Smith [28] showed that two shocks must exist in the nozzle starting process although the present data show three peaks. The reason for the third peak is not known at present but is attributed to flow establishment on the flat plate [29]. Three peaks are also seen in the heat transfer history obtained by East et al. [30]. Another observation is the flow establishment time. East et al. [30] thought that the establishment of a quasi-steady boundary-layer flow on the flat plate is similar to that which occurs in a shock tube, the latter problem having been addressed by Davies and Bernstein [31]. Present flow establishment data compare favorably with Davies and Bernstein's predictions, Fig. 9. The present data are also approximately predicted by criteria proposed by Lee and Lewis [32], with the predictions erring on the low side. Approximately 3 ms are required to establish flow on a 1 m long model if condition 5 is chosen, and a more "luxurious" establishment time is available if condition 5′ is chosen. The breakdown of the quasi-steady flow is also indicated in Fig. 8. The cause of this breakdown, whether due to the arrival of the driver gas or the arrival of an unsteady expansion reflected from the driver tube, cannot be determined from pressure mea-

surements. Surface heat flux measurements are currently being analyzed to determine more precisely the nature of this breakdown.

Present research activities

The shock tunnel has been used primarily for shock boundary-layer interaction studies so far. Two configurations have been examined, namely, a swept interaction generated by a fin [33] and a two-dimensional interaction of an external shock impinging near an expansion corner. Preceding these studies, the boundary layer over the test surface was also extensively investigated [34, 35]. In addition, an exploratory program to study slender delta wings at high angles of attack at a hypersonic Mach number is underway.

Conclusions

A small shock tunnel has been placed into operation at UTA for basic research into hypersonic flow problems. In addition to research, an important contribution of the facility is the academic training it affords. Innovative ways of achieving specific test requirements and of reducing the cost and difficulty of tunnel operations have been implemented.

Acknowledgements

The author would like to thank the faculty, staff and students of the ARC who contributed to the successful development and continued operation of the shock tunnel. In particular, the author would like to thank Messrs. K.-M. Chung and E.G. Pace for their efforts at surmounting innumerable problems to make the shock tunnel a viable research facility. Special thanks are also due to them for obtaining data used in this paper. In addition, the author enjoyed numerous, fruitful discussions with Dr. D.R. Wilson, who oversaw the initial development of the tunnel.

The author would also like to acknowledge with thanks the donations of equipment, namely, the 24 MPa compressor by the Army Aeroflightdynamics Laboratory; nozzles, test sections, diffusers and high-pressure storage vessel by LTV Aerospace and Defense Co. and the schlieren system by Bell Helicopters Textron. Thanks also go to the Dean of Engineering for the purchase of the high-speed data acquisition system. The support by NASA Langley through Grant NAG 1-891, monitored by Dr. J.P. Weidner, for research into hypersonic shock boundary-layer interactions is also gratefully acknowledged. Finally, the author expresses his gratitude to operators of short-duration facilities, too numerous to acknowledge individually, who readily shared their experiences and thoughts on the specialized requirements that are involved with such facilities.

References

[1] Wittliff, C.E., "A Survey of Existing Hypersonic Ground Test Facilities – North America," *Aerodynamics of Hypersonic Lifting Vehicles*, Paper 1, AGARD CP-428, 1987.

[2] Stalker, R.J., "Shock Tunnels for Real Gas Hypersonics," *Aerodynamics of Hypersonic Lifting Vehicles*, Paper 4, AGARD CP-428, 1987.

[3] Sharma, S.P. and Park, C., "Survey of Simulation and Diagnostic Techniques for Hypersonic Nonequilibrium Flows," *J. Thermophys.*, Vol. 4, 1990, pp. 129–142.

[4] Tamagno, J., Bakos, R., Pulsonetti, M. and Erdos, J., "Hypervelocity Real Gas Capabilities of GASL's Expansion Tube (HYPULSE) Facility," AIAA Paper 90-1390, 1990.

[5] Wilson, D.R., "Development of the University of Texas at Arlington Aerodynamics Research Center," AIAA Paper 88-2002, 1988.

[6] Stuessy, W.S., Murtugudde, R.G., Lu, F.K. and Wilson, D.R., "Development of the UTA Hypersonic Shock Tunnel," AIAA Paper 90-0080, 1990.

[7] Moore, J.A., "Description and Initial Operating Performance of the Langley 6-Inch Expansion Tube Using Heated Helium Driver Gas," NASA TM X-3240, 1975.

[8] Needham, D.A., Elfstrom, G.M. and Stollery, J.L., "Design and Operation of the Imperial College Number 2 Hypersonic Gun Tunnel," I.C. Aero Rep. 70-04, Imperial Coll., London, U.K., 1970.

[9] Gough, H. and Parker, J., *A Glossary of Terms Used in Heraldry*, Gale Research Co., Detroit, Michigan, 1966.

[10] Yamaki, Y. and Rooker, J.R., "Experimental Investigation of Circular, Flat, Grooved and Plain Steel Diaphragms Bursting into a 30.5-Centimeter Square Section," NASA TM X-2549, 1972.

[11] Chung, K.-M. and Lu, F.K., "Shock-Tube Calibration of a Fast-Response Pressure Transducer," AIAA Paper 90-1399, 1990.

[12] Gibson, B. and Dolling, D.S., "Wall Pressure Fluctuations Near Separation in a Mach 5, Sharp Fin-Induced Turbulent Interaction," AIAA Paper 91-0646, 1991.

[13] Trimmer, L.L., Matthews, R.K. and Buchanan, T.D., "Measurement of Aerodynamic Heat Rates at the Von Karman Facility," *ICIASF'73 Record*, 1973, pp. 35–44.

[14] Gai, S.L., Reynolds, N.T., Ross, C. and Baird, J.P., "Measurements of Heat Transfer in Separated High-Enthalpy Dissociated Laminar Hypersonic Flow Behind a Step," *J. Fluid Mech.*, Vol. 199, 1989, pp. 541–561.

[15] Roberts, G.T., private communication, Southampton University, U.K. 1990.

[16] Schultz, D.L. and Jones, T.V., "Heat Transfer Measurements in Short-Duration Hypersonic Facilities," AGARDograph 165, 1973.

[17] George, W.K., Rae, W.J. and Woodward, S.H., "An Evaluation of Analog and Numerical Techniques for Unsteady Heat Transfer Measurement with Thin-Film Gauges in Transient Facilities," *Experimental Thermal and Fluid Sci.*, Vol. 4, 1991, pp. 333–342.

[18] Edney, B.E., "Temperature Measurements in a Hypersonic Gun Tunnel Using Heat-Transfer Methods," *J. Fluid Mech.*, Vol. 27, 1967, pp. 503–512.

[19] Stalker, R.J., "Hypervelocity Aerodynamics with Chemical Nonequilibrium," *Ann. Rev. Fluid Mech.*, Vol. 21, 1989, pp. 37–60.

[20] Lukasiewicz, J., *Experimental Methods of Hypersonics*, Marcel Dekker, New York, 1973.

[21] Minucci, M.A.S. and Nagamatsu, H.T., "An Investigation of Hypersonic Shock Tunnel Testing at an Equilibrium Interface Condition of 4100 K: Theory and Experiment," AIAA Paper 91-1707, 1991.

[22] Wendt, J.F., "European Hypersonic Wind Tunnels," *Aerodynamics of Hypersonic Lifting Vehicles*, Paper 2, AGARD CP-428, 1987.

[23] Daum, F.L. and Gyarmathy, G., "Condensation of Air and Nitrogen in Hypersonic Wind Tunnels," *AIAA J.*, Vol. 6, 1968, pp. 458–465.

[24] Morrisette, E. L., Stone, D. R. and Cary, A. M., "Downstream Effects of Boundary Layer Trips in Hypersonic Flows," NASA SP 216, 1968.

[25] Arrington, J.P., Joiner, R.C., Jr. and Henderson, A., Jr., "Longitudinal Characteristics of Several Configurations at Hypersonic Mach Numbers in Conical and Contoured Nozzles," NASA TN D-2489, 1964.

[26] Johnson, C.B., "Pressure and Flow-Field Study at Mach Number 8 of Flow Separation on a Flat Plate with Deflected Trailing-Edge Flap," NASA TN D-4308, 1968.

[27] Hopkins, E.J., Jillie, D.W. and Sorensen, V.L., "Charts for Estimating Boundary-Layer Transition on Flat Plates," NASA TN D-5846, 1970.

[28] Smith, C.E., "The Starting Process in a Hypersonic Nozzle," *J. Fluid Mech.*, Vol. 24, 1966, pp. 625–640.

[29] Pace, E.G., "An Experimental Investigation of Hypersonic Swept Shock Boundary-Layer Interactions," M.S.A.E. Thesis, University of Texas at Arlington, 1991.

[30] East, R.A., Stalker, R.J. and Baird, J.P., "Measurements of Heat Transfer to a Flat Plate in a Dissociated High-Enthalpy Laminar Air Flow," *J. Fluid Mech.*, Vol. 97, 1980, pp. 673–699.

[31] Davies, W.R. and Bernstein, L., "Heat Transfer and Transition to Turbulence in the Shock-Induced Boundary Layer on a Semi-Infinite Flat Plate," *J. Fluid Mech.*, Vol. 36, 1969, pp. 87–112.

[32] Lee, J.Y. and Lewis, M.J., "A Numerical Study of the Flow Establishment Time in Hypersonic Shock Tunnels," AIAA Paper 91-1706, 1991.

[33] Pace, E.G. and Lu, F.K., "On the Scale of Surface Features in Hypersonic Swept Shock Boundary-Layer Interactions," AIAA Paper 91-1769, 1991.

[34] Chung, K.-M. and Lu, F.K., "An Experimental Study of a Hypersonic Cold-Wall Turbulent Boundary Layer," AIAA Paper 92-0312, 1992.

[35] Chung, K.-M. and Lu, F.K., "The Downstream Influence and Fluctuating Surface Pressure of Hypersonic Expansion Corner Flows," submitted to the 2nd Nat. Fluid Dyn. Cong., Los Angeles, June 22–25,1992.